

A Density Functional Theory Study on the Adsorption of Chlorobenzene on the Si(111)-7 × 7 Surface

Zhen-Hua Li, Yan-Cha Li, Wen-Ning Wang, Yong Cao, and Kang-Nian Fan*

Shanghai Key Laboratory of Molecular Catalysis & Innovative Materials, Department of Chemistry, Center for Theoretical Chemical Physics, Fudan University, Shanghai 200433, China

Received: May 26, 2004; In Final Form: July 2, 2004

The adsorption of chlorobenzene (CIPh) on the Si(111)-7 × 7 surface has been investigated with the B3LYP density functional method. All possible adsorption configurations of chlorobenzene have been investigated. Binding energies including zero-point vibrational energy correction of different adsorption configurations were calculated at the B3LYP/6-31G(d,p) level of theory. It was found that mono- σ binding states are very instable. They will quickly transfer to the more stable di- σ binding states. Upon heating, the di- σ bonded chlorobenzene will desorb and then break its C–Cl bond to form a Si–Cl bond. Upon further heating, the desorbed chlorobenzene will break the C–H bond to form a Si–H bond. All four types of bindings prefer the unfaulted half of the unit cell and the center-rest atom adsorption sites. The most stable di- σ binding state is a 2,5 binding configuration. The calculated binding energy for this configuration is 23.73 kcal mol⁻¹, in good agreement with the experimental desorption energy barrier of 23.30 kcal mol⁻¹.

1. Introduction

The adsorption of aromatic molecules on silicon surface plays an important role in photochemical etching for device fabrication^{1,2} or as precursors in low-temperature chemical vapor deposition (CVD) of diamond coatings on various nondiamond substrates.³ A detailed understanding of the binding state and adsorption mechanism of aromatic molecules with well-defined surfaces is of great importance in developing these industrial processes. These molecules are also often chosen as probing molecules to study the photon- or electron-induced chemistry of adsorbates on various surfaces of great industrial importance. The Si(111)-7 × 7 surface is ideal in this sense since it has rich and complex active sites and has been studied by various experimental and theoretical methods.⁴

As a prototype of aromatic molecules, the adsorption of benzene on the Si(111)-7 × 7 surface have been intensively studied both experimentally^{5–14} and theoretically.^{15–18} On the contrary, studies on the adsorption of substituted benzene molecules on the Si(111)-7 × 7 surface are scarce. Due to the substitution, the adsorption of substituted benzene molecules is much more complicated than that of benzene. Chen et al. have investigated the adsorption of chlorobenzene (CIPh) on Si(111)-7 × 7 at room temperature using scanning tunneling microscopy (STM).¹⁹ It was found that the center adatoms are more reactive than the corner adatoms, and the faulted half of the unit cell is more favored compared to the unfaulted side. Later, Polanyi et al. and Sloan et al. studied the electron-induced reaction of CIPh to the Si(111)-7 × 7 surface.^{20–22} Under the impact of electrons, they observed chemically bound chlorine atoms on the surface. Recently, Xu and co-workers have performed a systematic investigation of the adsorption of benzene, CIPh, and other substituted aromatic molecules on both clean and the deuterium-modified Si(111)-7 × 7 surface with HREELS and TDS.^{14,23–28} Their HREELS experiments provided

direct information regarding the structure of the chemisorbed molecules on the surface. Combined with the previous STM work and their own HREELS and TDS results, they proposed that the chemisorbed CIPh is stereoselectively di- σ bonded through its 2,5 carbon atoms to a pair of neighboring adatom and rest atom of the Si(111)-7 × 7 surface, yielding a 2,5-chlorocyclohexadiene-like complex.²³

It has been well established both experimentally and theoretically that the adsorption of benzene on the Si(111)-7 × 7 surface follows a precursor-mediated mechanism: the molecule is first physisorbed and later chemisorbed by transferring to a more stable di- σ binding state forming a cyclohexadiene-like complex. Recently, two theoretical works have studied one of the adsorption configurations of CIPh, a 1,4 di- σ configuration forming C1–Si and C4–Si bonds, on the Si(111)-7 × 7 surface.^{21,22} Jiang et al. have also studied the possible dissociation pathway of this di- σ configuration into chemically bonded phenyl and chlorine atom on the surface.²¹ No adsorption mechanism and other mono- σ type binding states as that of the adsorption of benzene have been systematically studied. The stereochemistry, the mechanism of the adsorption, and the modification of the adsorption on the electron structure of the surface have not been well understood. A systematic study on the adsorption of CIPh is undoubtedly helpful to understand the adsorption properties and mechanism of CIPh itself and other substituted benzene molecules as well.

2. Computational Details

On the Si(111)-7 × 7 surface, there are four types of adatoms, the corner and the center adatoms at the faulted half and unfaulted half of the unit cell, respectively, and two types of rest atoms, rest atoms at the faulted and unfaulted half of the unit cell, respectively. Therefore, four cluster models were used to model the different adsorption sites of the Si(111)-7 × 7 surface: **C**orner adatom and rest atom at the **u**nfaulted half (**CoU**) and **f**aulted half of the unit cell (**CoF**); **C**enter adatom and rest atom at the **u**nfaulted half (**CeU**) and **f**aulted half of

* To whom correspondence should be addressed. Fax: +86-21-65643977. E-mail: knfan@fudan.edu.cn.

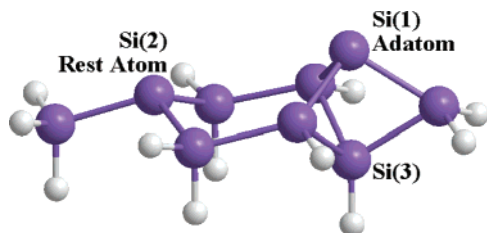


Figure 1. The silicon cluster model (Si_9H_{12}) used in the present study.

TABLE 1: Distances between Si Atoms (in Å) Used for the Bare Si_9H_{12} Cluster Shown in Figure 1^a

parameters	CeU	CoU	CeF	CoF
Si(1)–Si(2)	4.559	4.568	4.566	4.576
Si(1)–Si(2) \perp	1.060	1.100	1.090	1.130
Si(1)–Si(3)	2.494	2.534	2.524	2.564

^a From ref 29.

the unit cell (CeF). The four types of adsorption sites are modeled by a Si_9H_{12} cluster as shown in Figure 1, varying its geometry according to the experimental geometry of the corresponding adsorption site (Table 1).²⁹ Hydrogen atoms were used to terminate the dangling bonds except for the adatom and the rest atom. The Si–H bond was fixed to 1.5 Å. Only the two Si atoms on the top of the cluster were allowed to move during the optimization. A larger cluster model was not used in this study since our previous study on the adsorption of the benzene molecule showed that results obtained using a cluster model of Si_9H_{12} agree well with those using larger models.¹⁶

ClPh can form either one C–Si or two C–Si bonds with the Si(111)- 7×7 surface, i.e., mono- σ , and 2,5, 1,4, 1,2, 2,3, 3,4 di- σ binding states. For the mono- σ binding state, there are 8 types of possible binding configurations for each adatom–rest atom site (Figure 2). For 2,5 and 1,4 binding states, there are 4 types of possible binding configurations (Figure 3). Although there are 6 types of binding configurations for all the 1,2, 2,3, 3,4 binding states, we just considered one 3,4 binding configuration as shown in Figure 3 (3c-1), since due to a geometry mismatch these binding configurations are highly impossible and have not been observed in any experiments. The dissociative binding configurations, in which either the C–H or C–Cl bond of ClPh is broken to form a chemisorbed phenyl group and a H–Si or Cl–Si bond, are shown in Figure 4. For the dissociative binding states, only those breaking the C4–H bond were considered. Therefore, a total of $4(4 + 8 + 1 + 2 + 2) = 68$ binding configurations were generated. For each configuration, geometry optimization was first performed and then followed by harmonic vibrational frequency analysis. Binding energies (BEs) corrected by zero-point vibrational energy (ZPE) scaled by 0.9614³⁰ were calculated by $\text{BE} = E_{\text{ClPh}} + E_{\text{cluster}} - E_{\text{system}}$.

All the geometry optimizations and harmonic vibrational frequency calculations were performed with the B3LYP^{31–34} density functional method in combination with the 6-31G(d,p) basis set. For all the mono- σ binding states, the pure Si_9H_{12} clusters, and the transition states, unrestricted open-shell wave functions were used. All the calculations were completed with the Gaussian 98 suite of programs.³⁵

3. Results and Discussion

3.1. Mono- σ Binding States. The ZPE corrected binding energies of all mono- σ binding states are listed in Table 2. For the binding states shown in Figure 2 (2a-1 and 2a-2), after geometry optimization, we finally obtained two dissociated products, which will be discussed in Section 3.4.

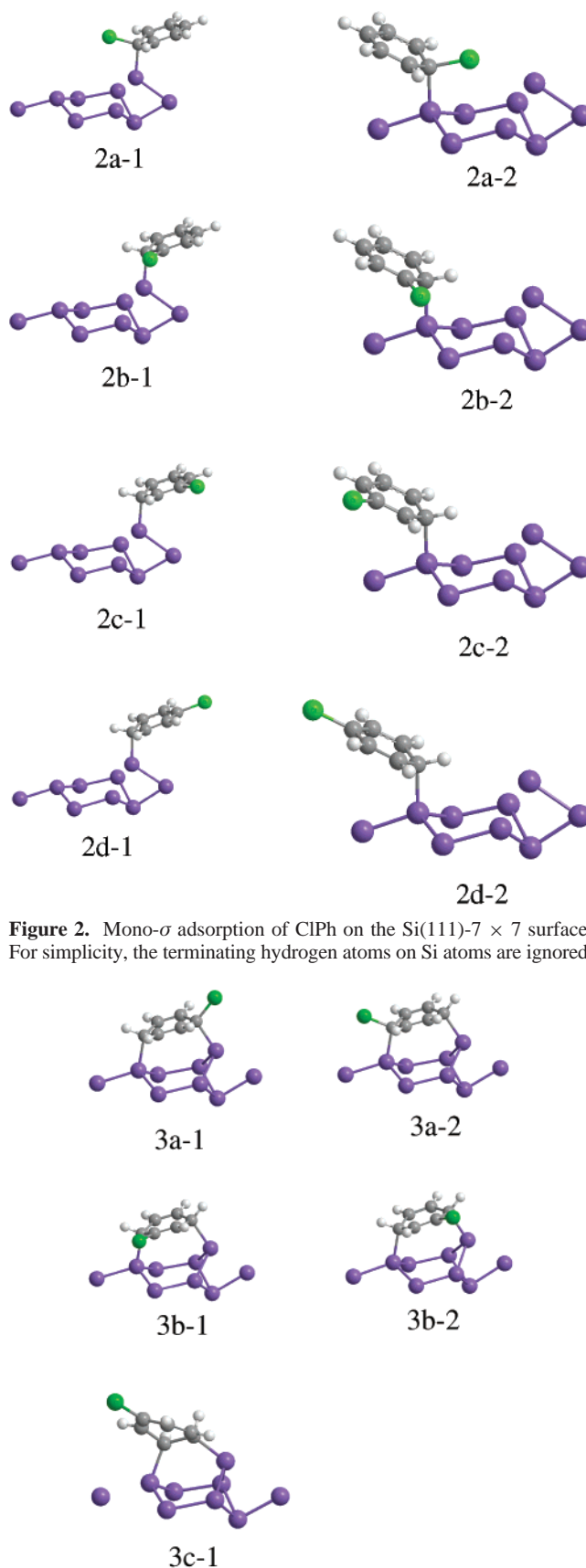


Figure 2. Mono- σ adsorption of ClPh on the Si(111)- 7×7 surface. For simplicity, the terminating hydrogen atoms on Si atoms are ignored.

Figure 3. Di- σ adsorption of ClPh on the Si(111)- 7×7 surface.

It is well-known that the reactivities of ortho, para, and meta carbon atoms of substituted benzene are different. However, which one is higher in activity depends not only on the substituent, but also on the attacking group itself. The chlorine

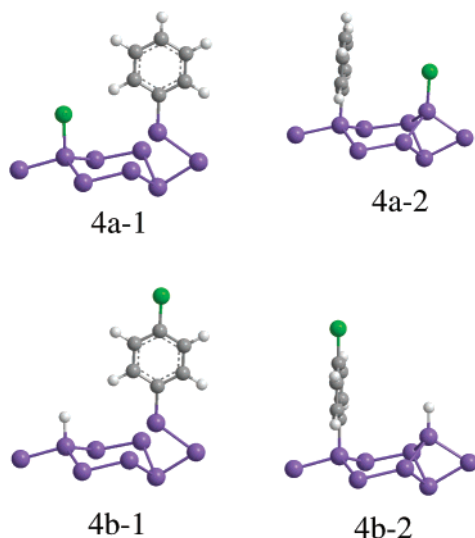


Figure 4. Dissociative binding states.

TABLE 2: Binding Energies (in kcal mol⁻¹) after ZPE Corrections of the Mono- σ Binding States

site	bond formed	adatom binding state	rest atom binding state
CeU	C2-Si	0.04	3.36
	C3-Si	2.42	3.63
	C4-Si	0.22	-4.92
CoU	C2-Si	0.16	-3.59
	C3-Si	0.10	1.04
	C4-Si	0.36	1.55
CeF	C2-Si	1.08	1.68
	C3-Si	0.78	1.96
	C4-Si	1.44	2.23
CoF	C2-Si	-1.48	-0.65
	C3-Si	-1.79	-0.38
	C4-Si	-1.12	-4.36

atom is a π electron provider and thus will make the C2 and C4 have more π electrons than C3. Therefore, a nucleophilic group will prefer to react with C3 rather than with C2 and C4 of CIPh. Table 2 shows that the reactivity of the dangling bond of the Si atom at the different adsorption site is different. For the CeU adsorption site, CIPh prefers to bind with the Si atom using the C3 atom. The most stable binding state is the binding of C3 with the rest atom of the surface. However, this binding configuration is not dominant since it is just slightly lower in energy than the binding configuration in which C2 is bonded to the rest atom (3.63 vs 3.36 kcal mol⁻¹). The binding of the C4 of CIPh with the rest atom of CeU is mostly disfavored in energy. On the contrary, for the CoU adsorption site, the binding between C4 and Si is slightly preferred in energy than other configurations. The binding of the C2 with the rest atom of CeU is mostly disfavored. For the faulted half of the surface, the binding of CIPh with CeF is similar to the binding with CoU, and it also slightly prefers to bind using the C4 atom. Unlike other adsorption sites, all the bindings between CIPh with CoF do not gain in energy. Similar to the binding of CIPh with CeU, the binding of C4 with the rest atom of CoF is mostly disfavored in energy.

Examination of Table 2 indicates that the most stable mono- σ binding configuration is the binding of CIPh to the rest atom of the center adatom–rest atom site (CeU or CeF). In our study on the adsorption of benzene it was also found that the binding of benzene to the rest atom is more stable than its binding to the adatom.¹⁶ Moreover, for each half, in general, the binding of CIPh to the center adatom–rest atom site is more stable than

TABLE 3: Binding Energies (in kcal mol⁻¹) after ZPE Corrections of the Di- σ Binding States

site	2,5 binding state	1,4 binding state	3,4 binding state ^e
CeU	23.73 ^a	21.13 ^c	-18.63
	22.80 ^b	21.29 ^d	
CoU	20.52 ^a	17.96 ^c	-24.17
	19.75 ^b	18.42 ^d	
CeF	20.06 ^a	19.49 ^c	-18.75
	21.12 ^b	19.71 ^d	
CoF	19.09 ^a	16.57 ^c	-19.37
	18.08 ^b	16.68 ^d	

^a C2 of CIPh is bonded to the adatom. ^b C2 of CIPh is bonded to the rest atom. ^c C1 of CIPh is bonded to the adatom. ^d C1 of CIPh is bonded to the rest atom. ^e C3 of CIPh is bonded to the rest atom.

that to the corner adatom–rest atom cluster. The former finding is in contradiction to our common sense that CIPh may be easier to access the outmost adatom. Careful examination of the Mulliken spin density on the two Si atoms indicates that in all the Si₉H₁₂ clusters the rest atom always has higher spin density than the adatom. For example, for the CeU cluster, the spin density on the rest atom is +0.970e, while that on the adatom is just -0.626e. Therefore, the rest atom is expected to be more reactive than the adatom.

3.2. Di- σ Binding States. The binding energies of all the di- σ binding states after ZPE corrections are collected in Table 3. Due to a geometry mismatch, 1,2, 2,3, and 3,4 di- σ binding configurations are all very high in energy. The energies of all four 3,4 binding configurations we considered here are higher than those of the free reactants by more than 18 kcal mol⁻¹ (Table 3). In these configurations, to match the short C3–C4 distance, the distance between the adatom and the rest atom is greatly shortened, from 4.56–4.58 Å (Table 1) to 3.85–3.87 Å. Similar to the mono- σ bindings, the 3,4 binding of CIPh with the CeU site is the strongest, and the binding to the center adatom–rest atom site is preferred. In a recent theoretical work, Lu et al. reported a 1,2 adsorption configuration formed between benzene and the Si(111)-7 × 7 surface. This configuration is slightly lower in energy than the free reactants.¹⁸ However, they relaxed all the Si atoms during the geometry optimization, resulting in a very short adatom–rest atom distance shortened by more than 1 Å than the ordinary distance (Table 1), which perhaps is impossible in the real surface reactions. Fixing the bottom layer atoms in modeling surface reactions by using cluster and slab models is probably more realistic.

The binding energies of 1,4 and 2,5 di- σ binding configurations are much larger than those of mono- σ and 3,4 di- σ binding configurations. Examination of Table 3 shows that for each half of the unit cell, the binding of CIPh with the center adatom–rest atom site (CeU or CeF) is more stable than the binding with the corner adatom–rest atom site (CoU or CoF), in good agreement with the observation of Polanyi et al.^{19,20} The authors pointed out that this preference of CeU/CeF over CoU/CoF may be due to the local electron density or the strain energy difference between the center adatom and corner adatom.¹⁹ An early theoretical calculation on the Si(111)-7 × 7 surface indicates that center adatoms have slightly larger local density of states above the Fermi level.³⁶ This is in accordance with the present study. The spin density on the center adatom of the unfaulted half is -0.626e, whereas it is -0.620e on the corner adatom. For the faulted half, the spin density is -0.629e on the center adatom and -0.619e on the corner adatom. Since the adsorption of CIPh and benzene molecules is more likely a radical addition process with surface Si atoms acting as a

radical,¹⁸ via a stepwise mechanism, more spin density on the attacking Si atoms will certainly result in a more stable binding state.

The binding of ClPh with the CeU site is the most stable in all the binding configurations, for both 2,5 and 1,4 bindings. This is very similar to the adsorption of benzene. The STM experiments of Polanyi and co-workers indicate that ClPh prefer to adsorb on the unfaulted half when the occupation number of the half unit cell is below 3, which is the number of rest atoms per half unit cell.^{19–21} Since the di- σ adsorption of ClPh uses two Si atoms, 3 is the highest number of ClPh di- σ bonded to a half unit cell. Therefore, it seems when the coverage is low, ClPh prefers to adsorb on the unfaulted half. The preference of the faulted over the unfaulted half under higher coverage may be due to a cooperative enhancement between the adsorbed ClPh molecules. Unfortunately, due to the limited computational power, it is still prohibitively expensive to calculate the adsorption of more than one ClPh molecule on the complex Si(111)-7 \times 7 surface.

Furthermore, for the 2,5 binding states, the calculated binding energies are even very close to the binding energies of benzene with the four types of adsorption sites (23.39, 20.20, 21.69, and 18.65 kcal mol⁻¹ for binding with CeU, CoU, CeF, and CoF, respectively).¹⁶ It seems that the substitution of the chlorine atom does not have a substantial effect on the binding energy of the benzene ring. However, due to the substitution effect, the adsorption of ClPh shows a slight preference of 2,5 binding over 1,4 binding, in agreement with the experimental work of Cao et al.²³ The slightly larger binding energy of the most stable binding configuration for ClPh than that for benzene (23.73 vs 23.39 kcal mol⁻¹) is in good agreement with the TDS experimental results of Cao et al., where they found that the desorption peak of ClPh is \sim 20 K higher than that of benzene.²³

The binding energy for the most stable binding configuration, a 2,5 binding state, is 23.73 kcal mol⁻¹. This is in very good agreement with the experimental results of Cao et al., where the desorption energy barrier they obtained for the chemisorbed ClPh is 23.30 kcal mol⁻¹.²³ If the energy barrier for the transfer of the precursor to this chemisorbed 2,5-chlorocyclohexadiene-like surface adduct is very low, the desorption energy barrier can be directly compared with our theoretical binding energy. In our calculations, it was indeed found that the energy barrier to form the mono- σ binding states and the energy barrier for its subsequent transfer to the more stable di- σ binding states is very low. We will discuss this in more detail in Section 3.4.

The agreement between the experimental binding energy and the present theoretical result is better than the earlier calculation of Jiang et al., where they calculated one 1,4 binding configuration using the ONIOM(B3LYP/3-21G*:HF/3-21G*)^{37,38} method with a much larger 5-layer cluster model with 3 adatoms (2 center and 1 corner).²¹ The binding energy they obtained is just 10.84 kcal mol⁻¹, about half of the experimental value. In a subsequent theoretical study on the adsorption of the benzene molecule on the Si(111)-7 \times 7 surface using a smaller 3-layer cluster model with B3LYP/6-31G(d) method, they obtained a binding energy of 22.37 kcal mol⁻¹,¹⁷ in good agreement with the previous experimental results^{14,39} and other theoretical results.^{16,18} This indicates that the size of the cluster plays a less important role in calculating the binding energy of aromatic molecules on the Si(111) surface. A cluster model with one adatom and one rest atom is good enough.

We have calculated the harmonic vibrational frequencies of the most stable 2,5 and 1,4 binding states, which were obtained by setting the atom weight of the Si atoms (except the adatom

TABLE 4: Binding Energies (in kcal mol⁻¹) after ZPE Corrections of the Dissociative Binding States Breaking the C–Cl Bond

adsorption site	Cl on adatom	Cl on rest atom
CeU	89.58	90.89
CoU	82.27	81.88
CeF	87.87	89.20
CoF	87.39	88.51

TABLE 5: Binding Energies (in kcal mol⁻¹) after ZPE Corrections of the Dissociative Binding States Breaking the C–H Bond

adsorption site	H on adatom	H on rest atom
CeU	57.30	60.17
CoU	54.72	57.60
CeF	55.60	58.46
CoF	55.12	57.98

and the rest atom) and the terminating H atoms to an arbitrary 1000.0 atomic unit to eliminate the effect of the Si–Si vibration and the terminating Si–H vibration. The vibrational frequencies are tabulated in Table S1 of the Supporting Information. Compared with the experimental vibrational modes observed in the HREELS experiment,²⁸ the vibrational frequencies of the 2,5 binding state are closer to experimental values. Nevertheless, the vibrational frequencies between the two binding states show no big difference except for a few vibrational modes, such as the C–Cl stretching (657 vs 593 cm⁻¹), C–Si stretching (671 vs 721 cm⁻¹), out-of-plane sp²-CH bending (842 vs 793 cm⁻¹), out-of-plane sp²-CH bending (1042 vs 973 cm⁻¹), and sp³-CH stretching (2977 vs 3053 cm⁻¹) modes. Among the five vibrational modes, the only experimental observed mode is the very strong out-of-plane sp²-CH bending mode at 862 cm⁻¹, which is one of the strongest vibrational modes calculated for the 2,5 binding state (842 cm⁻¹) while the strongest mode is calculated for the 1,4 binding state (793 cm⁻¹). The better agreement between the theoretical vibrational spectrum of the 2,5 binding state and experimental results indicates that the 2,5 binding is indeed the dominant configuration of the adsorption of ClPh. However, due to the closeness of the vibrational spectrums and also the binding energies of the two binding states, one cannot rule out the existence of the less favorable 1,4 binding configurations.

3.3. Dissociative Binding States. Results for breaking C–Cl and C–H bonds are tabulated in Tables 4 and 5, respectively.

For the binding states obtained by cleaving the C–Cl bond or the C–H bond, the geometries of the configurations with the chlorine/hydrogen atom chemically bonded to the rest atom are different from those of the configurations with the chlorine/hydrogen atom bonded to the adatom (Figure 4). In the formal binding configurations, the chlorine/hydrogen atom and the phenyl group are coplanar, with the C2–H bond of the phenyl group pointing toward the chlorine/hydrogen atom. On the other hand, in the later configurations, the chlorine/hydrogen atom is facing the phenyl plane. It is possible that the weak interaction between the π orbital of the phenyl group and the charged chlorine/hydrogen atom, which is common between ions and aromatic rings, plays an important role in these resulting configurations.

Compared with mono- σ and di- σ binding states, the binding energies of the dissociative binding states are much larger in value, simply due to the retaining of the aromatic benzene ring in the dissociative binding states. The dissociation of the C–Cl bond is most exothermic, for which the calculated binding energies are between 82 and 90 kcal mol⁻¹. On the other hand, the dissociation of the C–H bond is less exothermic, whose

TABLE 6: Energy Barriers (in kcal mol⁻¹) to Form Binding Configurations on the Center Adatom–Rest Atom Adsorption Site of the Unfaulted Half^a

	product to form (transition state)					
	mono- σ (Figure 5a)	2,5 di- σ (Figure 5b)	3,4 di- σ (Figure 5c)	C–Cl breaking (Figure 5d)	C–Cl breaking (Figure 5e)	C–H breaking (Figure 5f)
energy barrier	0.41	-2.09	22.73	3.42	3.73	20.14

^a All energy barriers are ZPE corrected and are all relative to the energy of the free reactants.

binding energies are between 54 and 58 kcal mol⁻¹. This is not unexpected since breaking a C–H bond is known to need much more energy than breaking a C–Cl bond.

The two types of dissociative binding states both show a similar trend that the configurations with the hydrogen/chlorine bonded to the rest atom are preferred over states with the hydrogen/chlorine bonded to the adatom. The only exception is the dissociative binding of ClPh to the CoU site. For both types of dissociative binding states, the configuration with the hydrogen/chlorine bonded to the rest atom of the CeU site is the most stable state. Similar to the mono- σ and di- σ adsorptions, the dissociative bindings energetically prefer the unfaulted half of the unit cell. In the experiment of photon-induced dissociation of ClPh, Jiang et al. found that after photon irradiation, the coverage on the faulted half decreases much more rapidly than that on the unfaulted half,²¹ indicating the desorption of ClPh from the unfaulted half is more difficult than that from the faulted half. However, the final coverage of the faulted half is still slightly higher. This is due to the “localized atomic reaction” nature of the dissociation induced by photon irradiation,²⁰ thus the dissociated fragments would bind to the faulted half first and then diffuse to the energetically preferred unfaulted half on condition that adequate energy is provided. However, one should take the comparison between the present theoretical results and the experimental results of the electron- or photon-induced dissociation of ClPh with care,^{20–22} since the dissociation under these experimental conditions may involve excited states or the negatively charged surface species, whereas the present theoretical results are better to be compared with thermal dissociation experimental results.

3.4. Dynamics. The adsorption of ClPh is similar to the adsorption of the benzene molecule, following a stepwise mechanism. A Diels–Alder-like reaction mechanism simultaneously forming two C–Si σ -bonds seems unlikely to exist since we could not obtain any TSs for this pathway. ClPh molecules will first bind to the surface to form mono- σ binding states. Then, the mono- σ binding states will transfer to the more stable 1,4 and 2,5 di- σ binding states. We have optimized the TS to form the most stable mono- σ binding state in which the C3 atom of the ClPh forms the C–Si bond with the unfaulted half (Figure 5a). The energy barrier to form this mono- σ binding state at 0 K is just 0.41 kcal mol⁻¹ (Table 6). Energy barriers to form other less stable mono- σ binding states will be slightly higher according to the Bell–Evans–Polanyi principle.⁴⁰ The energy barrier from mono- σ binding states to di- σ binding states is very low. The energy of the transition state (Figure 5b) to form the most stable 2,5 binding state (with ClPh bonded to center adatom–rest atom adsorption site of the unfaulted half) is actually lower than that of the free reactants (the surface and the ClPh molecule) by 2.09 kcal mol⁻¹. Thus, the formation of the 1,4 and 2,5 di- σ binding states is almost barrierless. The mono- σ binding states on the pathway are very unstable intermediates, with too short a lifetime to be captured by the present experimental techniques.

The formation of the 1,2, 2,3, 3,4 di- σ binding states is unfavorable both kinetically and thermodynamically. The

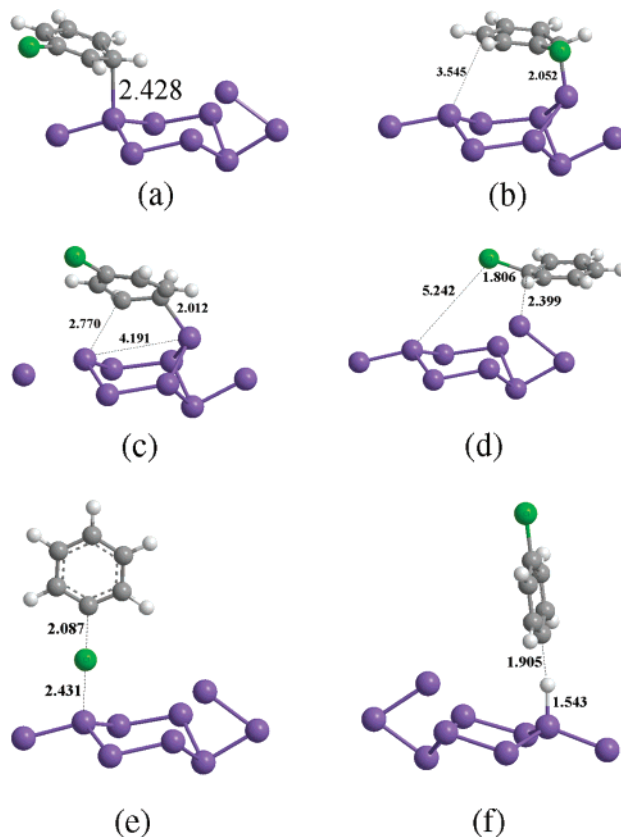


Figure 5. Transition structures. Bond lengths shown are in Å.

optimized transition structure to form the most stable 3,4 di- σ binding state is shown in Figure 5c. In this TS, the Si1–Si2 distance is greatly shortened. Its relative energy to the free reactants is very high, 22.73 kcal mol⁻¹. On the other hand, the barrier for the 3,4 di- σ binding state to release ClPh is just 4.10 kcal mol⁻¹ (Tables 3 and 6). Therefore, these di- σ binding states are unstable both kinetically and thermodynamically, and cannot be observed.

Upon further heating, electron impact, or photon irradiation, as have been shown by experimental studies, di- σ binding states can be transferred to dissociative binding states. There are two possible pathways for this process. The first one is a desorption–readsorption mechanism, in which chemically adsorbed molecules will first desorb, then break the C–Cl/C–H bond to form dissociative binding states directly from the gas-phase ClPh. The second one is a direct dissociation mechanism in which the Cl or H atom is abstracted by the neighboring adatoms or rest atoms as proposed by Jiang et al.²¹

For the first pathway, we have obtained two TSs to break the C–Cl bond: a second-order TS as shown by Figure 5d and a true TS as shown by Figure 5e. In the former second-order TS, the C–Cl bond is stretched from 1.761 to 1.806 Å. The forming C–Si bond is 2.399 Å. This second-order TS is calculated to be 3.42 kcal mol⁻¹ at 0 K above the free reactants. Slightly shortening the C–Si bond and optimizing the structure

will finally produce a dissociative binding state as shown in Figure 4 (4a-1). This is the reason we could not obtain mono- σ binding configurations as shown in Figure 2 (2a-1 and 2a-2). The later true TS looks more like an atom abstraction TS by radicals common in organic reactions. The breaking C–Cl bond is stretched from 1.761 to 2.087 Å, longer than the former second-order TS. The forming C–Si bond is 2.431 Å, also longer. This TS is higher in energy at 0 K than the reactants by 3.73 kcal mol⁻¹, slightly higher than the former second-order TS. Nevertheless, both TSs are higher in energy than the TS forming the mono- σ binding state, which will transfer to the more stable 1,4 or 2,5 di- σ binding state smoothly without energy barrier. The 3 kcal mol⁻¹ energy difference between the TS breaking C–Cl bond and the TS forming mono- σ binding state guarantees the adsorption of ClPh under mild conditions exclusively forms 1,4 and 2,5 di- σ binding states.

A similar TS breaking C–H bond as the abstraction of chlorine atom from ClPh by the Si atom has also been optimized (Figure 5f). In this TS, the benzene ring is facing the adatom, slightly tilting toward the adatom. The breaking C–H bond is stretched very long, to 1.905 Å, whereas the forming Si–H bond is just 1.543 Å, close to the length of the ordinary Si–H bond. Compared to other TSs previously optimized, the energy barrier to break the C–H bond is much higher, reaching 20.14 kcal mol⁻¹ (Table 6). Thus, the direct breaking of the C–H bond is the least favorable pathway in energy.

As for the second pathway, due to the limitation of the present cluster model, we cannot optimize the TS breaking the C–Cl/C–H bond from the di- σ binding states to the dissociative binding states. Jiang et al. have approximately located a TS for the cleavage of the C–Cl bond from a 1,4 di- σ binding configuration. The energy barrier is about 44 kcal mol⁻¹, which is about 33 kcal mol⁻¹ above the free reactants.²¹ In viewing the underestimation of the binding energy for the di- σ binding state by the method they used, the actual energy barrier may be higher. The estimated energy barrier for breaking the C–H bond of a di- σ bonded benzene is slightly higher, about 36 kcal mol⁻¹ above the free reactants at the AM1 level.¹⁷ Both values are much higher than the energy barriers we calculated. Thus, the transfer of the 1,4 and 2,5 di- σ binding states to the dissociative binding states by heating more likely involves a desorption–readsorption mechanism. In the HREELS study of the adsorption of ClPh, Cao et al. did observe the cleavage of the C–Cl bond after heating the surface at 400 K, a temperature 20 K above the desorption peak of the TDS.²³ As the electron- and photon-induced cleavage of the C–Cl bond and the C–H bond may involve excited states or negatively charged species, we will not compare our theoretical results regarding the dynamics of the cleavage with the experiments of Polanyi et al.^{20,21} and Sloan et al. here.²²

4. Conclusions

In summary, the adsorption of ClPh on the Si(111)-7 × 7 surface will first form mono- σ binding states, which will quickly transfer to more stable 1,4 and 2,5 di- σ binding states. The 1,2, 2,3, and 3,4 di- σ binding states are unstable both kinetically and thermodynamically. For the di- σ bindings, ClPh prefers the unfaulted half of the unit cell under low coverage. The most stable di- σ binding configuration is a 2,5 binding with the center adatom–rest atom site of the unfaulted half. Upon heating, the 1,4 and 2,5 di- σ bonded ClPh molecules will desorb, and then break the C–Cl bond via a chlorine abstraction TS by the radical-like surface Si atom. The dissociated ClPh molecules also prefer to bind to the unfaulted half of the unit cell and the

center adatom–rest atom sites. Upon further heating, the desorbed ClPh molecules will break their C–H bond, forming a Si–H bond and chemisorbed phenyl group. Our calculation results are in good agreement with available experimental results.

Acknowledgment. This work is supported by the National Natural Science Foundation of China (20273015), the Natural Science Foundation of Shanghai Science and Technology Committee (02DJ14023), and the Major State Basic Research Development Program (2003CB615807).

Supporting Information Available: Table of selected harmonic vibrational frequencies. This material is available free of charge via the Internet at <http://pubs.acs.org>.

References and Notes

- (1) Flaum, H. C.; Sullivan, D. J. D.; Kummel, A. C. *J. Phys. Chem.* **1994**, *98*, 1719–1731.
- (2) Wolkow, R. A. *Annu. Rev. Phys. Chem.* **1999**, *50*, 413–441.
- (3) Schmidt, I.; Benndorf, C. *Diamond Relat. Mater.* **1998**, *7*, 266–271.
- (4) Buke, C. B. *Chem. Rev.* **1996**, *96*, 1237–1259.
- (5) Taguchi, Y.; Fujisawa, M.; Nishijima, M. *Chem. Phys. Lett.* **1991**, *178*, 363.
- (6) Taguchi, Y.; Ohta, Y.; Katsumi, T.; Ichikawa, K.; Aita, O. *J. Electron Spectrosc. Relat. Phenom.* **1998**, *88*, 671.
- (7) Macpherson, C. D.; Hu, D. Q.; Leung, K. T. *Solid State Commun.* **1991**, *80*, 217–220.
- (8) Macpherson, C. D.; Leung, K. T. *Phys. Rev. B* **1995**, *51*, 17995.
- (9) Carbone, M.; Piancastelli, M. N.; Zanoni, R.; Comtet, G.; Dujardin, G.; Hellner, L. *Surf. Sci.* **1998**, *407*, 275–281.
- (10) Carbone, M.; Piancastelli, M. N.; Casaletto, M. P.; Zanoni, R.; Comtet, G.; Dujardin, G.; Hellner, L. *Phys. Rev. B* **2000**, *61*, 8531–8536.
- (11) Brown, D. E.; Moffatt, D. J.; Wolkow, R. A. *Science* **1998**, *279*, 542.
- (12) Kawasaki, T.; Sakai, D.; Kishimoto, H.; Akbar, A. A.; Ogawa, T.; Oshima, C. *Surf. Interface Anal.* **2001**, *31*, 126.
- (13) Tomimoto, H.; Takehara, T.; Fukawa, K.; Sumii, R.; Sekitani, T.; Tanaka, K. *Surf. Sci.* **2003**, *526*, 343.
- (14) Cao, Y.; Wei, X. M.; Chin, W. S.; Lai, Y. H.; Deng, J. F.; Bernasek, S. L.; Xu, G. Q. *J. Phys. Chem. B* **1999**, *103*, 5698.
- (15) Wang, Z. H.; Cao, Y.; Xu, G. Q. *Chem. Phys. Lett.* **2001**, *338*, 7–13.
- (16) Li, Y. C.; Wang, W. N.; Cao, Y.; Fan, K. N. *Acta Chim. Sin.* **2002**, *60*, 653–659.
- (17) Petsalakis, I. D.; Polanyi, J. C.; Theodorakopoulos, G. T. *Surf. Sci.* **2003**, *544*, 162–169.
- (18) Lu, X.; Wang, X.; Yuan, Q.; Zhang, Q. *J. Am. Chem. Soc.* **2003**, *125*, 7923–29.
- (19) Chen, X. H.; Kong, Q.; Polanyi, J. C.; Rogers, D.; So, S. *Surf. Sci.* **1995**, *340*, 224–230.
- (20) Lu, P. H.; Polanyi, J. C.; Rogers, D. *J. Chem. Phys.* **1999**, *111*, 9905–9907.
- (21) Jiang, G. P.; Polanyi, J. C.; Rogers, D. *Surf. Sci.* **2003**, *544*, 147–161.
- (22) Sloan, P. A.; Hedouin, M. F. G.; Palmer, R. E. *Phys. Rev. Lett.* **2003**, *91*, 118301.
- (23) Cao, Y.; Deng, J. F.; Xu, G. Q. *J. Chem. Phys.* **2000**, *112*, 4759–4767.
- (24) Cao, Y.; Yong, K. S.; Wang, Z. Q.; Chin, W. S.; Lai, Y. H.; Deng, J. F.; Xu, G. Q. *J. Am. Chem. Soc.* **2000**, *120*, 1812–1813.
- (25) Cao, Y.; Wang, Z. H.; Deng, J. F.; Xu, G. Q. *Angew. Chem., Int. Ed.* **2000**, *39*, 2740–2743.
- (26) Qiao, M. H.; Cao, Y.; Deng, J. F.; Xu, G. Q. *Chem. Phys. Lett.* **2000**, *325*, 508–512.
- (27) Qiao, M. H.; Tao, F.; Cao, Y.; Li, Z. H.; Dai, W. L.; Deng, J. F.; Xu, G. Q. *J. Chem. Phys.* **2001**, *114*, 2766–2774.
- (28) Cao, Y.; Yong, K. S.; Wang, Z. H.; Deng, J. F.; Lai, Y. H.; Xu, G. Q. *J. Chem. Phys.* **2001**, *115*, 3287–3296.
- (29) Tong, S. Y.; Huang, H.; Wei, C. M.; Packard, W. E.; Men, F. K.; Glander, G.; Webb, M. B. *J. Vac. Sci. Technol. A* **1988**, *6*, 615.
- (30) Scott, A. P.; Radom, L. *J. Phys. Chem.* **1996**, *100*, 16502–16513.
- (31) Becke, A. D. *J. Chem. Phys.* **1993**, *98*, 5648–5652.
- (32) Lee, C.; Yang, W.; Parr, R. G. *Phys. Rev. B* **1988**, *37*, 785–789.
- (33) Vosko, S. H.; Wilk, L.; Nusair, M. *Can. J. Phys.* **1980**, *58*, 1200–1211.

(34) Stephens, P. J.; Devlin, F. J.; Chabalowski, C. F.; Frisch, M. J. *J. Phys. Chem.* **1994**, *98*, 11623–11627.

(35) Frisch, M. J.; Trucks, G. W.; Schlegel, H. B.; Scuseria, G. E.; Robb, M. A.; Cheeseman, J. R.; Zakrzewski, V. G.; Montgomery, J. A., Jr.; Stratmann, R. E.; Burant, J. C.; Dapprich, S.; Millam, J. M.; Daniels, A. D.; Kudin, K. N.; Strain, M. C.; Farkas, O.; Tomasi, J.; Barone, V.; Cossi, M.; Cammi, R.; Mennucci, B.; Pomelli, C.; Adamo, C.; Clifford, S.; Ochterski, J.; Petersson, G. A.; Ayala, P. Y.; Cui, Q.; Morokuma, K.; Malick, D. K.; Rabuck, A. D.; Raghavachari, K.; Foresman, J. B.; Cioslowski, J.; Ortiz, J. V.; Stefanov, B. B.; Liu, G.; Liashenko, A.; Piskorz, P.; Komaromi, I.; Gomperts, R.; Martin, R. L.; Fox, D. J.; Keith, T.; Al-Laham, M. A.; Peng, C. Y.; Nanayakkara, A.; Gonzalez, C.; Challacombe, M.; Gill, P. M. W.; Johnson, B.; Chen, W.; Wong, M. W.; Andres, J. L.; Gonzalez, C.;

Head-Gordon, M.; Replogle, E. S.; Pople, J. A. *Gaussian 98*, revision A.7; Gaussian, Inc.: Pittsburgh, PA, 1998.

(36) Brommer, K. D.; Galvan, M.; Dal Pino, A., Jr.; Joannopoulos, J. D. *Surf. Sci.* **1994**, *314*, 57–70.

(37) Svensson, M.; Humbel, S.; Froese, R. D. J.; Matsubara, T.; Sieber, S.; Morokuma, K. *J. Phys. Chem.* **1996**, *100*, 19357–19363.

(38) Dapprich, S.; Komaromi, I.; Byun, K. S.; Morokuma, K.; Frisch, M. J. *J. Mol. Struct. (THEOCHEM)* **1999**, *461*, 1–20.

(39) Wolkow, R. A.; Moffatt, D. J. *J. Chem. Phys.* **1995**, *103*, 10696–10700.

(40) Dewar, M. J. S. *The Molecular Orbital Theory for Organic Chemistry*; McGraw-Hill: New York, 1969.